Review of Different Speed Estimation schemes for Sensorless Induction Motor Drives

M. S. Zaky, M. Khater, H. Yasin, and S. S. Shokralla

Electrical Engineering Dept., Faculty of Engineering, Minoufiya University, Shebin El-Kom, Egypt
Address correspondence to *Mohamed Shaban Zaky*, Electrical Engineering Dept., Faculty of Engineering, Minoufiya University, Shebin El-Kom, Egypt.
Tel.: 002-0482329988*; fax:* 002-0482235695
E-mail: m_s_zaky@yahoo.com

Abstract

Induction motor drives without direct speed sensors have the features of low cost, high reliability, better noise immunity and less maintenance requirements. Therefore, there is a great interest in the research community to develop a high performance induction motor drive that does not require a direct speed sensor for its operation; that is to develop a speed-sensorless induction motor drive. The information required for rotor speed estimation is extracted from measured stator voltages and currents at the motor terminals. Different speed estimation algorithms are used for this purpose. The main concerns regarding speed estimation are related to steady state accuracy, dependency on motor parameters, estimation bandwidth and dynamic behavior. This paper presents a comprehensive study of the different speed estimation techniques and their corresponding merits and demerits as well as their feasibility for estimating the rotor speed. The different speed estimation methods are compared according to a proposed set of criteria which allow assigning the merits that can be used to choose the proper method, depending on the specific application.

Keywords: Induction Motor, Sensorless, Speed Estimation Methods

1. INTRODUCTION

High performance electric motor drives are considered an essential requirement for modern industrial applications. In the past, dc motors have been widely used for this purpose. However, large size, heavy weight and frequent maintenance requirements make dc motors

an expensive solution. Moreover, mechanical commutator-brush assembly cause undesired sparking, which is not allowed in certain applications. These inherent drawbacks of dc motors have prompted continual attempts to find out a better solution for the problem. Numerous attempts have been made to use induction motors instead of dc ones since they have many advantages like simplicity, reliability, low cost and virtually maintenance-free. However, the high nonlinearity and time-varying nature of an induction motor drive demands fast switching power devices and a large amount of real-time computation [1].

Precise speed and torque control of an induction motor is now possible due to the recent developments in power electronics and digital signal processors (DSP) using *field oriented control* technique. There are essentially two general methods of field oriented control namely the *direct* and *indirect methods*. The *direct method* depends on generating unit vector signals, required for flux orientation, from the flux signals obtained by measurement or estimation. The *indirect field oriented method* uses the rotor speed and the slip angular frequency derived from the rotor dynamic equations to generate the unit vector signals to achieve flux orientation. Although indirect field orientation method is very sensitive to motor parameters, such as rotor time constant, it is generally preferred than the direct one. This is because direct method requires machine disassembly and modification to insert search coils or Hall-effect sensors for flux measurement. Moreover the fragility of flux sensors often degrades the inherent robustness of the induction motor drive [1].

2. SPEED-SENSORLESS CONTROL

Accurate speed information is always necessary to realize high performance and high-precision speed control of induction motor drives. Conventionally, a direct speed sensor, such as an encoder, is usually mounted to the motor shaft to measure its speed. The use of such direct speed sensors implies additional electronics, extra wiring, extra space, frequent

maintenance and careful mounting which detracts from the inherent robustness and reliability of the drive. Also, it adds an extra cost and the drive system becomes expensive. For these reasons, the development of alternative indirect methods becomes an important research topic [5]. Therefore, there is a great interest in the research community to develop a high performance induction motor drive that does not require a direct speed sensor for its operation; in other words, to develop a speed-sensorless induction motor drive. Many advantages are expected from speed-sensorless induction motor drives such as reduced hardware complexity, low cost, reduced size, elimination of direct sensor wiring, better noise immunity, increased reliability, and less maintenance requirements. Speed-sensorless motor drives are also preferred in hostile environments and high-speed applications [6]

The positive features of speed-sensorless systems introduces them as a preferable choice for the next generation of commercial motor drives, not only for induction machines but also include other electrical machines, such as switched reluctance motors (SRM) and permanent-magnet synchronous motors [2-4].

3. SPEED ESTIMATION SCHEMES OF SENSORLESS INDUCTION MOTOR DRIVES

Recently, serious attempts to eliminate direct speed sensor of induction motor drives are reported. All these attempts employ motor terminal variables and its parameters in some way or another to estimate the speed. The question always arises is *to which extent the method is successful without deteriorating the dynamic performance of the drive.*

Several methods have been recently, proposed for speed estimation of high performance induction motor drives. Some of these methods are based on a non-ideal phenomenon such as rotor slot harmonics [5-9]. Such methods require spectrum analysis, which besides being time consuming procedures; they allow a narrow band of speed control. Another class of algorithms relies on some kind of probing signals injected into stator terminals (voltage

and/or current) to detect the rotor flux and consequently, the motor speed [10-14]. These probing signals, sometimes, introduce a high frequency torque pulses, and hence speed ripple. In some cases a useful data may be distorted due to interference with the high frequency probing signals.

Despite the merits of the above methods of speed estimation near zero speed, they suffer from large computation time, complexity and limited bandwidth control. Alternatively, speed information can be obtained by using the machine model and its terminal quantities, like voltage and current [15-36]. These include different methods such as the use of simple open loop speed calculators [6-7]; Model Reference Adaptive Systems (MRAS) [15-19]; Extended Kalman Filters [20-22], Adaptive Flux Observer [23-27]; Artificial Intelligence Techniques [28-31]; and Sliding Mode Observer (SMO) [32-36]. Model-based methods are characterized by their simplicity and good performance at high speeds; however they exhibit lower accuracy at low speeds mostly, due to parameter variations. Figure 1 shows a chart of the different speed estimation methods for sensorless systems.

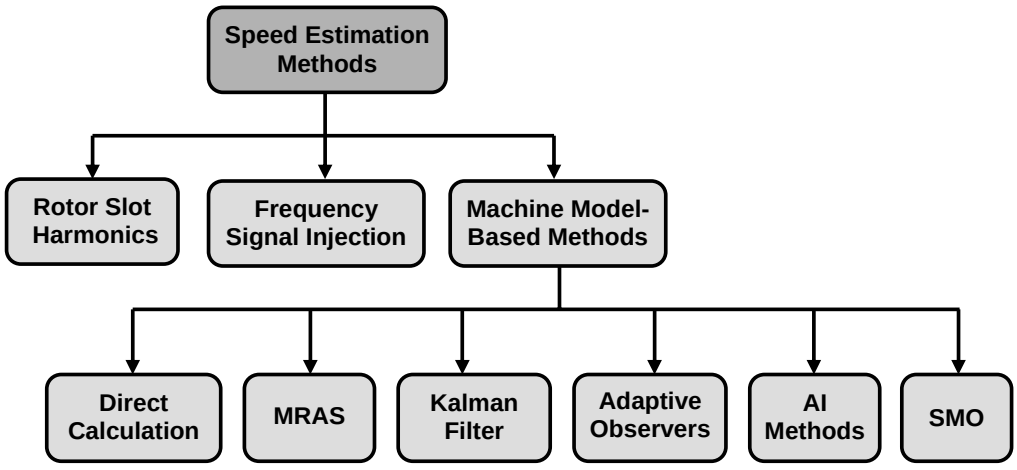

Fig. 1 Speed estimation methods of sensorless systems.

In this paper, different speed estimation techniques of sensorless induction motor drives are reviewed and discussed. The object is to classify speed-sensorless schemes with emphasizing the merits and demerits for each method. A comparison between different speed estimation methods based on a devised set of criteria is introduced. The problems of low

speed operation and parameter adaptation associated with speed-sensorless systems are introduced. In most cases a tradeoff emerges between the implementation simplicity and the overall behavior. However, the result is considered a useful tool to justify a certain scheme for a specific application. A brief explanation of speed estimation schemes for sensorless induction motor drives is introduced below.

3.1. Rotor Slot Harmonics (RSH) Method

The method of speed estimation is based on detecting space harmonics induced by rotor slots [5-9]. The rotor slots generate space harmonic components in the air gap magneto motive force (mmf) that modulate the stator flux linkage at a frequency proportional to the rotor speed, and to the number of rotor slots N_r. Since N_r is generally not a multiple of three, the rotor slot harmonics induce harmonic voltages in the stator phases

$$v_{sl} = \hat{v}_{sl} \sin(N_r \omega_r \pm \omega_s)\tau, \quad \text{where } N_r = 3n \mp 1, \quad n=1, 2, 3, ... \tag{1}$$

that appear as triplen harmonics with respect to the fundamental stator voltage v_{sl}. As all triplen harmonics from zero sequence systems, they can be easily separated from the much larger fundamental voltage. The zero sequence voltage v_o is the sum of the three phase voltages in a wye-connected stator winding

$$v_o = \frac{1}{3}(v_a + v_b + v_c) \tag{2}$$

When adding the phase voltages, all non-triplen components, including the fundamental, get cancelled while the triplen harmonics add up. To isolate the signal that represents the mechanical angular velocity ω_r of the rotor, a band pass filter is employed having its central frequency adaptively tuned to the rotor slot harmonic frequency $N_r\omega_r + \omega_s = 2\pi/\tau_{sl}$ in Eqn. (1).

The block diagram of speed estimation based on rotor slot harmonics is shown in Fig. 2. The adaptive band pass filter extracts the rotor slot harmonics signal v_{sl}. The filtered signal is digitized by detecting its zero crossing instants t_z. A software counter is incremented at each zero crossing by one count to memorize the digitized rotor position angle ϑ. A slot frequency signal is then obtained by digital differentiation in the same way as from an incremental encoder. The accurate rotor speed ω_r is subsequently computed with reference to Eqn. (1) [5].

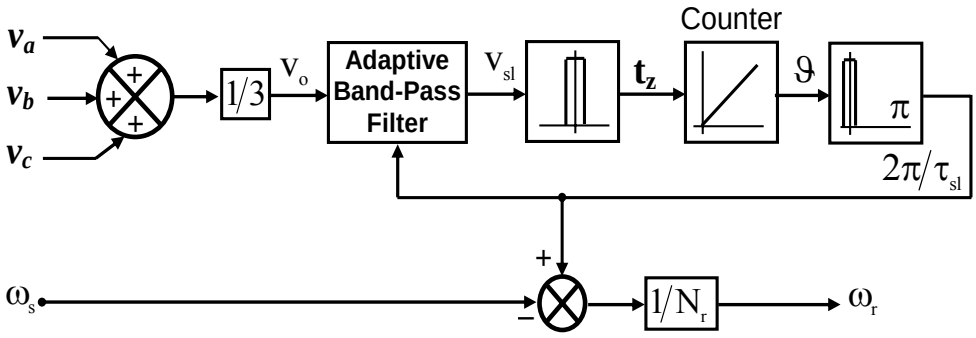

Fig. 2 Block diagram of speed estimation based on rotor slot harmonics.

As mentioned earlier, this approach needs high precision measurements which increase the hardware/software complexity. Also, they suffer from large computation time, complexity and limited bandwidth control.

3.2. Frequency Signal Injection (FSI) Method

Speed estimation scheme in the method is based on signal injection. A high frequency voltage signal, superimposed on the fundamental voltage, is typically used to excite the anisotropic phenomena of the motor and the rotor position or flux direction is identified from the current response. This paid for the presence of significant torque (and, therefore, speed) ripple. Also, the signal carrying useful information may be distorted due to interference with other signals of the same kind. Furthermore, a common drawback of signal-injection methods is that their dynamic response is usually only moderate [10-14].

Figure 3 shows the basic structure of speed estimation using frequency signal injection method. An estimated field angle $\hat{\delta}$ is used to perform current control in field coordinates. A revolving carrier frequency ω_c is injected through the voltage signal $v_c = v_c e^{j\omega_c t}$. The carrier frequency components in the measured machine currents are attenuated by a Low Pass Filter (LPF) in the feedback path of the current controller. A Band Pass Filter (BPF) extracts the carrier generated current vector $\boldsymbol{i_c}$. The rotor speed can be estimated using Phase-Locked loop (PLL) [5].

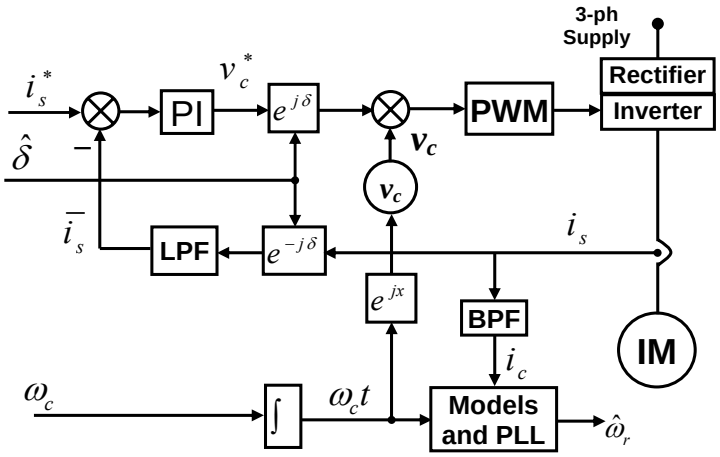

Fig. 3 speed estimation based on signal injection.

3.3. Machine Model (MM) Methods

A great deal of research interest is given to the third category of speed estimation, which is based on machine model, for its simplicity. In this category, the motor terminal variables and its parameters are used in some way to estimate its operating speed. This category can be classified according to the algorithm used for speed estimation. Some details of machine model based methods of speed estimation can be summarized as follows:

3.3.1. Direct calculation method (DCM)

Direct calculation method of speed estimation for induction motor is characterized by its simplicity and small computational time. Speed estimation scheme is based on a rotor flux

estimation process. The procedure of rotor speed estimation can be summarized as follows [6-7]:

First, the rotor flux in stationary reference frame is estimated based on the measured stator voltages and currents using Eqn. (3) and Eqn. (4).

$$\frac{d\lambda_{qr}^{s}}{dt}=\frac{L_r}{L_m}v_{qs}^{s}-\frac{L_r}{L_m}\left(R_s i_{qs}^{s}+\sigma L_s\frac{di_{qs}^{s}}{dt}\right) \tag{3}$$

$$\frac{d\lambda_{dr}^{s}}{dt}=\frac{L_r}{L_m}v_{ds}^{s}-\frac{L_r}{L_m}\left(R_s i_{ds}^{s}+\sigma L_s\frac{di_{ds}^{s}}{dt}\right) \tag{4}$$

$$p\lambda_{qr}^{s}=\frac{L_m}{T_r}i_{qs}^{s}+\omega_r\lambda_{dr}^{s}-\frac{1}{T_r}\lambda_{qr}^{s} \tag{5}$$

$$p\lambda_{dr}^{s}=\frac{L_m}{T_r}i_{ds}^{s}-\omega_r\lambda_{qr}^{s}-\frac{1}{T_r}\lambda_{dr}^{s} \tag{6}$$

Second, the angle θ_e of the rotor flux vector λ_r in relation to the d-axis of the stationary frame is defined as follows:

$$\theta_e=\omega_e t=\tan^{-1}\frac{\lambda_{qr}^{s}}{\lambda_{dr}^{s}} \tag{7}$$

where

$$\left.\begin{aligned}\lambda_{qr}^{s}&=\left|\hat{\lambda}_r\right|\sin\omega_e t\\ \lambda_{dr}^{s}&=\left|\hat{\lambda}_r\right|\cos\omega_e t\end{aligned}\right\} \tag{8}$$

$$\dot{\theta}_e=\omega_e=\frac{\lambda_{dr}^{s}\dot{\lambda}_{qr}^{s}-\lambda_{qr}^{s}\dot{\lambda}_{dr}^{s}}{\lambda_{dr}^{s\,2}+\lambda_{qr}^{s\,2}} \tag{9}$$

Substituting Eqns. (5) and (6) in Eqn. (9); the estimated rotor speed becomes;

$$\hat{\omega}_r=\frac{1}{\hat{\lambda}_r^2}\left[\left(\lambda_{dr}^{s}\dot{\lambda}_{qr}^{s}-\lambda_{qr}^{s}\dot{\lambda}_{dr}^{s}\right)-\frac{L_m}{T_r}\left(\lambda_{dr}^{s}i_{qs}^{s}-\lambda_{qr}^{s}i_{ds}^{s}\right)\right] \tag{10}$$

where; $\hat{\lambda}_r^{2}=\lambda_{dr}^{s\,2}+\lambda_{qr}^{s\,2}$

Therefore, given a complete knowledge of the motor parameters, the instantaneous speed ω_r can be calculated from Eqn. (10). This process is illustrated in the block diagram of Fig. 4.

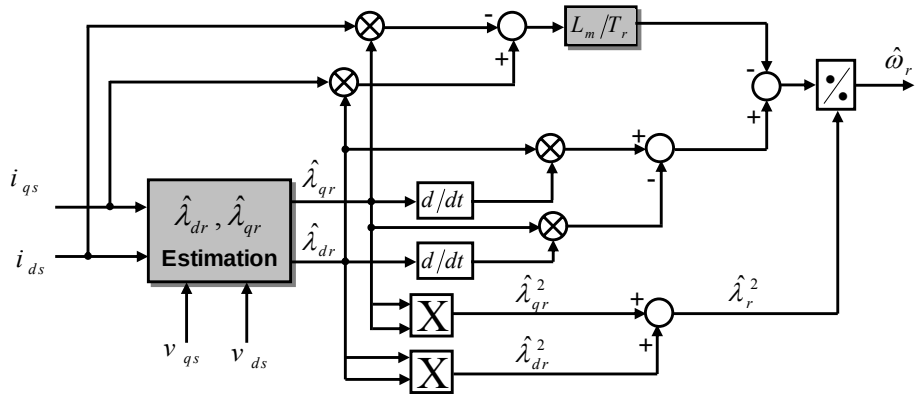

Fig. 4 Block diagram of rotor speed estimation structure based on direct calculation method.

As shown from the block diagram, the rotor flux estimation is essential for rotor speed estimation. There are three problems related to the rotor flux estimation;

1. The first is the need of ideal integral,
2. The second one is its sensitivity to parameters variation specially stator resistance R_S which has large influence at very low speed, and
3. The third one is the use of the actual stator voltage which is difficult to measure due to the PWM and the influence of dead-time.

These problems become more serious as the frequency speed approaches zero.

3.3.2. Model reference adaptive system

Model Reference Adaptive System (MRAS) is one of the famous speed observers usually used for sensorless induction motor drives. It is one of many promising techniques employed in adaptive control. Among various types of adaptive system configuration, MRAS is important since it leads to relatively easy-to-implement systems with high speed of adaptation for a wide range of applications. One of the most noted advantages of this type of adaptive system is its high speed of adaptation. This is due to the fact that a measurement of the difference between the outputs of the reference model and adjustable model is obtained

directly by the comparison of the states (or outputs) of the reference model with those of the adjustable system. The block ‘‘reference model’’ represents demanded dynamics of actual control loop. The block ‘‘adjustable model’’ has the same structure as the reference one, but with adjustable parameters instead of the unknown ones as shown in Fig. 5.

The MRAS speed estimation structure consists basically of *a reference model*, *adjustable model* and *an adaptive mechanism*. *The reference model*, which is independent of the rotor speed, calculates the state variable, x , from the terminal voltage and current. *The adjustable model*, which is dependent on the rotor speed, estimates the state variable, $\hat{x}$. *The error* ε between calculated and estimated state variables is then used to drive an adaptation mechanism which generates the estimated speed, $\hat{\omega}_r$, for the adjustable model as shown in the block diagram of Fig. 5.

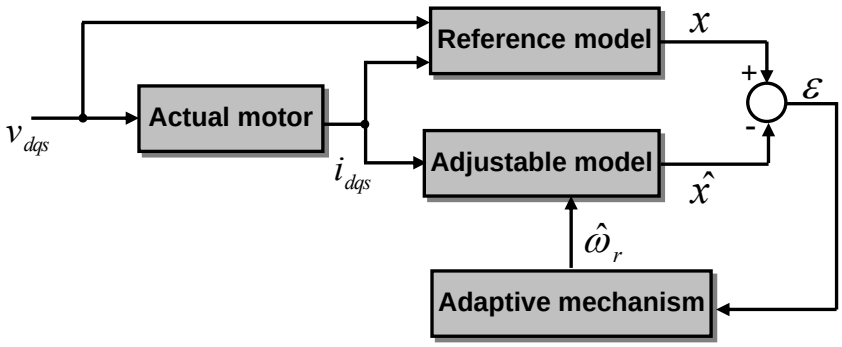

Fig. 5 Rotor speed estimation structure using MRAS.

It should be noted that, speed estimation methods using MRAS can be classified into various types according to the state variable. The most commonly used are the rotor flux-based MRAS, back emf-based MRAS, and stator current-based MRAS.

1. Rotor Flux-Based MRAS

In the rotor flux-based MRAS, *the rotor flux* is used as an output value for the model to estimate the rotor speed. As shown, when the rotor flux of *the adjustable model* (Eqn. (12)) is in accordance with that of *the reference model* (Eqn. (11)), the rotor speed of the adjustable model represents the real motor speed [15-16].

$$\frac{d\lambda_r^s}{dt} = \frac{L_r}{L_m}\left(v_s^s - R_s i_s^s - \sigma L_s \frac{di_s^s}{dt} \right) \tag{11}$$

$$\frac{d\hat{\lambda}_r^s}{dt} = j\hat{\omega}_r \hat{\lambda}_r^s - \frac{1}{T_r}\hat{\lambda}_r^s + \frac{L_m}{T_r} i_s^s \tag{12}$$

Figure 6 shows the block diagram of speed estimation algorithm using rotor flux based MRAS. The rotor speed estimated by this method is expressed as;

$$\hat{\omega}_r = K_P\left(\lambda_{qr}^s \hat{\lambda}_{dr}^s - \lambda_{dr}^s \hat{\lambda}_{qr}^s\right) + K_I \int \left(\lambda_{qr}^s \hat{\lambda}_{dr}^s - \lambda_{dr}^s \hat{\lambda}_{qr}^s\right) dt \tag{13}$$

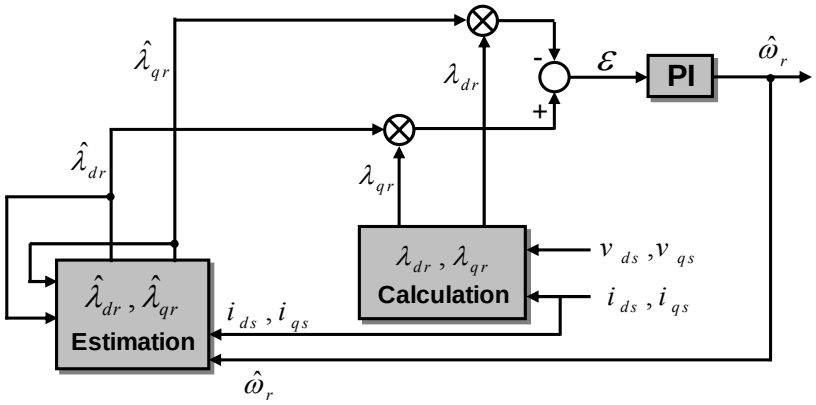

Fig. 6 Rotor speed estimation structure using rotor flux based MRAS.

In rotor flux based MRAS, the presence of an open integration in the stator leads to problems with initial conditions and drift. A low pass filter may be used instead of the pure integration; however, it has a degrading effect on speed estimation at low speeds and introduces a time delay.

2. Back emf-Based MRAS

The model reference adaptive approach, if based on back emf rather than the rotor flux, offers an alternative to avoid the problems involved with open integration. The open integration is circumvented in this approach and, other than in the MRAS based on the rotor flux, there are no low-pass filters that create a bandwidth limit. A more severe source of inaccuracy is a possible mismatch of the reference model parameters, particularly of the stator resistance [16-18].

$$e = v_s^s - R_s i_s^s - \sigma L_s \frac{d i_s^s}{dt} \tag{14}$$

$$\hat{e} = \frac{L_m}{L_r}\left[j\hat{\omega}_r \left(L_m i_s^s + L_r i_r^s \right) - R_r i_r^s \right] \tag{15}$$

The back emf **e** is calculated from the reference model based on the terminal voltage and current, while $\hat{e}$ is the back emf estimated from the adjustable model. Figure 7 shows the block diagram of speed estimation using back emf based MRAS. The rotor speed estimated by this method is expressed as;

$$\hat{\omega}_r = K_P \left(e_q \hat{e}_d - e_d \hat{e}_q \right) + K_I \int \left(e_q \hat{e}_d - e_d \hat{e}_q \right) dt \tag{16}$$

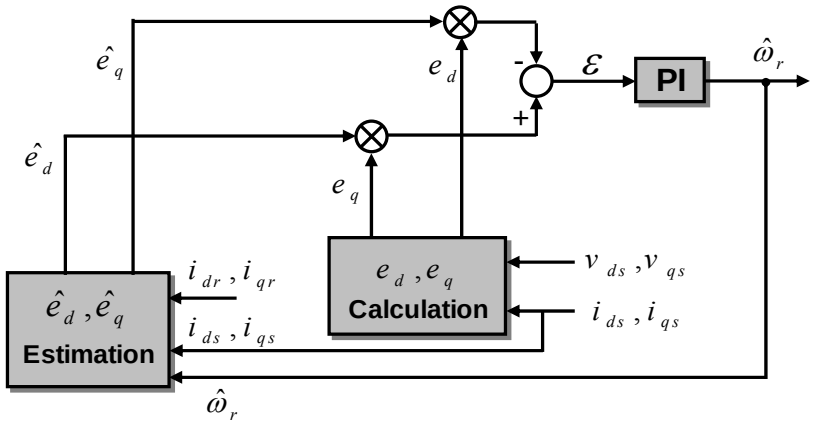

Fig. 7 Rotor speed estimation structure using back EMF based MRAS.

3. Stator Current-Based MRAS

For the aforementioned reasons, *stator current* may be used as an output value for MRAS speed estimation model. The rotor speed is estimated according to this method using the rotor flux which is expressed in terms of the stator voltage, stator current and motor parameters.

The rotor speed is estimated according to this method using the rotor flux which is expressed in terms of the stator voltage, stator current and motor parameters as [19];

$$\lambda_{dr}^s = \frac{L_r}{L_m}\left[\int \left(v_{ds}^s - R_s i_{ds}^s \right) dt - \sigma L_s i_{ds}^s \right] \tag{17}$$

$$\lambda_{qr}^{s} = \frac{L_r}{L_m}\left[\int\left(v_{qs}^{s} - R_s i_{qs}^{s}\right)dt - \sigma L_s i_{qs}^{s}\right] \tag{18}$$

Using the rotor flux and motor speed, the stator current is represented as;

$$i_{ds}^{s} = \frac{1}{L_m}\left(\lambda_{dr}^{s} + \omega_r T_r \lambda_{qr}^{s} + T_r \frac{d\lambda_{dr}^{s}}{dt}\right) \tag{19}$$

$$i_{qs}^{s} = \frac{1}{L_m}\left(\lambda_{qr}^{s} - \omega_r T_r \lambda_{dr}^{s} + T_r \frac{d\lambda_{qr}^{s}}{dt}\right) \tag{20}$$

Using Eqn. (19) and Eqn. (20), and estimated speed, the stator current is estimated as;

$$\hat{i}_{ds}^{s} = \frac{1}{L_m}\left(\lambda_{dr}^{s} + \hat{\omega}_r T_r \lambda_{qr}^{s} + T_r \frac{d\lambda_{dr}^{s}}{dt}\right) \tag{21}$$

$$\hat{i}_{qs}^{s} = \frac{1}{L_m}\left(\lambda_{qr}^{s} - \hat{\omega}_r T_r \lambda_{dr}^{s} + T_r \frac{d\lambda_{qr}^{s}}{dt}\right) \tag{22}$$

From the relationship between the calculated stator current and the estimated stator current, the difference in the stator current is obtained as;

$$i_{ds}^{s} - \hat{i}_{ds}^{s} = \frac{T_r}{L_m}\lambda_{qr}^{s}\left(\omega_r - \hat{\omega}_r\right) \tag{23}$$

$$\hat{i}_{qs}^{s} - i_{qs}^{s} = \frac{T_r}{L_m}\lambda_{dr}^{s}\left(\omega_r - \hat{\omega}_r\right) \tag{24}$$

If Eqn. (23) and Eqn. (24) are multiplied by the rotor flux and added together, then the following expression can be obtained;

$$\left(i_{ds}^{s} - \hat{i}_{ds}^{s}\right)\lambda_{qr}^{s} + \left(\hat{i}_{qs}^{s} - i_{qs}^{s}\right)\lambda_{dr}^{s} = \frac{T_r}{L_m}\left(\omega_r - \hat{\omega}_r\right)\left(\lambda_{dr}^{s\,2} + \lambda_{qr}^{s\,2}\right) \tag{25}$$

As a result of Eqn. (25), the error of the rotor speed can be written as;

$$\omega_r - \hat{\omega}_r = n\left[\left(i_{ds}^{s} - \hat{i}_{ds}^{s}\right)\lambda_{qr}^{s} + \left(\hat{i}_{qs}^{s} - i_{qs}^{s}\right)\lambda_{dr}^{s}\right] \tag{26}$$

where, $n = \frac{L_m}{T_r} \frac{1}{\left[\left(\lambda^s_{dr} \right)^2 + \left(\lambda^s_{qr} \right)^2 \right]}$

Figure 8 shows a block diagram of the stator current-based MRAS method. From Eqn. (26), the speed estimation error is determined from the stator current and rotor flux. This error is continuously reduced to zero by using a PI controller with appropriate proportional and integral gains. In Eqn. (26), the magnitude of the rotor flux is maintained as constant, as in general vector control. On the other hand, this method can produce a fast convergence and exact speed estimation, since the stator current error is represented as a function of the first degree of the speed estimation error.

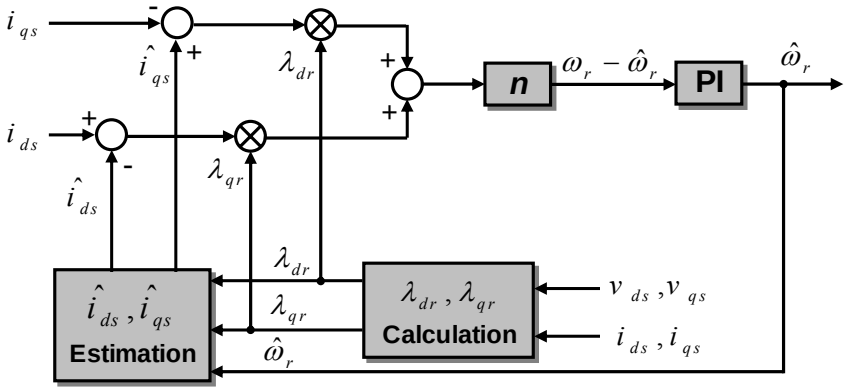

Fig. 8 Configuration of speed estimation scheme using stator current based MRAS.

In MRAS methods using the rotor flux and back EMF, the relationship between the model error and the speed estimation error is unclear; therefore, the MRAS controller gain has a nonlinear characteristic. As a result, these methods are difficult to estimate speed in a low speed region and at zero-speed owing to the increment of this nonlinear characteristic [15-18]. Whereas in stator current based MRAS, the stator current error is represented as a function of the first degree for the error value in the speed estimation. Therefore, this method can produce fast speed estimation and is robust to variations in the parameter error. In addition, it offers a considerable improvement in the performance of a sensorless vector controller at a low speed [19].

The main advantages of MRAS algorithms are they robustness, fast convergence and small computation time. The main drawbacks of MRAS algorithms are their sensitivity to inaccuracies in the reference model, and difficulties of designing the adaptation mechanism block. Selection of adaptive mechanism gains is a compromise between achieving fast response and high robustness against noise and disturbances affecting the system.

3.3.3. Kalman filter approach

Kalman filter (KF) algorithm is suitable to the system which has many unknown noises such as current ripple by PWM, noise by modeling error, measurement error, and so forth. Those noises are treated as a disturbance in Kalman filter algorithm. In real system, some uncertainties in the model and environment as modeling inaccuracies, disturbances and noises should be considered [20-22].

State equations with random noises can be given as;

$$\frac{dx(t)}{dt} = Ax(t) + Bu(t) + G(t) \quad (27)$$

$$y(t) = Cx(t) + \nu(t) \quad (28)$$

where x(t), u(t), and y(t) represent, respectively, the state variables, the commands variables and the output variables, $G(t)$ and $\nu(t)$ are the input noise and output noise, respectively.

For nonlinear problems, the KF is not strictly applicable since linearity plays an important role in its derivation and performance as an optimal filter. The Extended Kalman Filter (EKF) attempts to overcome this difficulty by using a linearized approximation where the linearization is performed about the current state estimate. This process requires the discretization of Eqns. (27) and (28) as;

$$x(k+1) = A(k)x(k) + B(k)u(k) + G(k) \quad (29)$$

$$y(k) = C(k)x(k) + \nu(k) \quad (30)$$

The Kalman filter algorithm is given by [20]:

$$P(0) = \mathrm{Var}\{x(0)\} \tag{31}$$

$$\hat{x}(0) = E\{x(0)\} \tag{32}$$

$$P(k+1) = A(k)P(k)A^{T}(k) + Q \tag{33}$$

$$\hat{x}(k+1) = A(k)\hat{x}(k) + B(k)u(k) \tag{34}$$

$$K(k+1) = P(k+1)C^{T}(k)\left[C(k)P(k+1)C^{T}(k) + R\right]^{-1} \tag{35}$$

$$\hat{x}(k+1/k) = \hat{x}(k+1) + K(k+1)\left[y(k) - C(k)\hat{x}(k+1)\right] \tag{36}$$

where Var(x) = the variance of x, E(x) = the expectation of x, K(k+1) = the Kalman gain matrix, P(k) = error covariance matrix, y(k) = the estimated output. The matrix Q means the disturbances such as the error produced by transforming into sampled data system. The error produced by the imperfection of current controller, and modeling error. The matrix R describes the noise produced by transforming the estimated output into sampled data model.

Figure 9 shows a typical structure of a Kalman filtering approach. The inputs to the plant are fed into a prediction model. The output of the plant is compared with the output from the model, and the resulting error is fed into a correction Kalman gain stage to reduce the error in the estimated states from the prediction model.

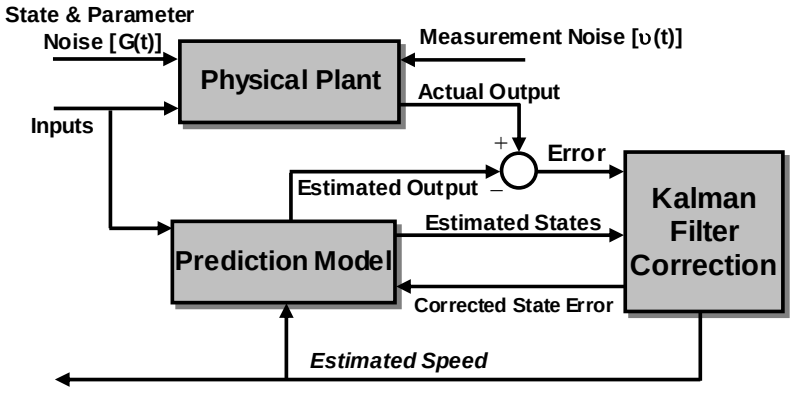

Fig. 9 Kalman filter structure for speed estimation.

The Kalman Filter approach has some inherent disadvantages, such as the influence of computation burden, and the absence of design and tuning criteria. Also, it is relatively

complicated and requires much more powerful microprocessors.

3.3.4. Adaptive flux observer

Adaptive flux observers (AFO) are also used for speed estimation of induction motor drives. The structure of an adaptive observer is basically composed of three main parts: an induction-motor model, observer's feedback gains, and a rotor speed adaptation mechanism as shown in Fig. 10. The characteristic of the speed estimation is governed by the assignment of the observer's feedback gains and PI gains adaptation mechanism [23-27].

An induction motor can be described, in a reference frame rotating with the angular velocity, by the following equations:

$$\frac{d}{dt}\begin{bmatrix}\lambda_s\\ \lambda_r\end{bmatrix}=\begin{bmatrix}A_{11} & A_{12}\\ A_{21} & A_{22}\end{bmatrix}\begin{bmatrix}\lambda_s\\ \lambda_r\end{bmatrix}+\begin{bmatrix}B_1\\ 0\end{bmatrix}\begin{bmatrix}v_s^s\end{bmatrix}=Ax+Bv_s \tag{37}$$

$$i_s = Cx \tag{38}$$

where A_{11}, A_{12}, A_{21}, A_{22}, B_1 and C are given in the Appendix.

The adaptive flux observer, that estimates both stator and rotor fluxes, is given by the following equations;

$$\begin{aligned}\frac{d\hat{x}}{dt} &= \hat{A}\hat{x} + Bv_s + K\left(\hat{i}_s - i_s\right)\\ \hat{i}_s &= C\hat{x}\end{aligned} \tag{39}$$

The estimated rotor speed obtained by adaptive flux observer based on Lyapunov theory is as follows:

$$\hat{\omega}_r = K_p\left[\hat{\lambda}_{qs}\cdot\left(\hat{i}_{ds}-i_{ds}\right)-\hat{\lambda}_{ds}\left(\hat{i}_{qs}-i_{qs}\right)\right]+K_I\int\left[\hat{\lambda}_{qs}\cdot\left(\hat{i}_{ds}-i_{ds}\right)-\hat{\lambda}_{ds}\left(\hat{i}_{qs}-i_{qs}\right)\right]dt \tag{40}$$

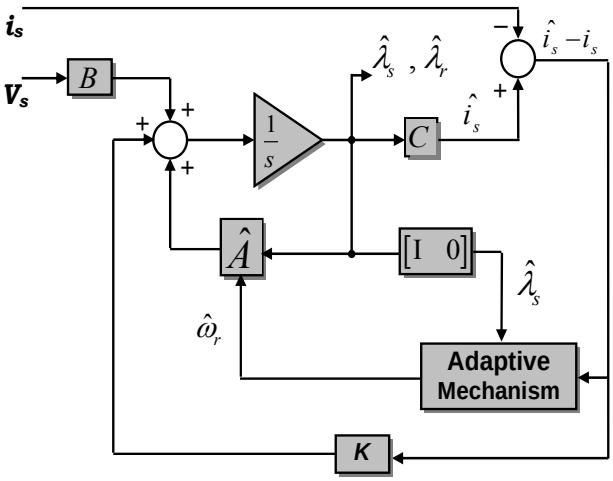

Fig. 10 Block diagram of the adaptive observer for speed estimation.

The feedback gain ***K*** is chosen to ensure global stability, and robust dynamic performance of the closed loop observer. A pole-placement approach is employed, and the choice of the desired pole locations is usually a compromise between achieving fast response and retaining high robustness against noise and disturbances affecting the system. The adaptation gains are selected by trial and error or by considering the root locus of the linearized model. Practically, the designer normally needs some guidelines to determine how the adaptation gains should be designed to obtain the required specification of tracking performance and sensitivity to noises.

The influence of parameter deviations and the low-speed and standstill operations are the most critical aspects affecting the accuracy of this method. Also, the difficulty encountered in the design of the feedback gain and the adaptation mechanisms are other problems.

The methods, based on the machine model, stated earlier exhibit accurate and robust speed estimation performance; however they are highly dependent on machine parameters. The induction motor is a highly coupled, nonlinear dynamic plant, and its parameters vary with time and operating conditions. Therefore, it is very difficult to obtain good performance for an entire speed range and transient states using previous methods. For these reasons, alternative speed estimation methods based on *artificial intelligence techniques* are proposed

for speed sensorless induction motor drives. These methods may achieve robustness and high performance with parameter variations.

3.3.5. Artificial intelligence techniques

The use of Artificial Intelligence (AI) to identify and control nonlinear dynamic systems has been proposed because they can approximate a wide range of nonlinear functions to any desired degree of accuracy. Moreover, they have the advantages of immunity from input harmonic ripples and robustness to parameter variations. Recently, there have been some investigations into the application of AI to power electronics and ac drives, including speed estimation [28-31].

Two well-known voltage and current models for rotor flux are necessary to estimate the speed of an induction motor using an NN. Since the induction motor voltages and currents are measured in the stationary reference frame, it is convenient to express these equations in the stationary frame, and they are expressed in Eqns. (41) and (42) as follows [31]:

$$p\begin{bmatrix}\lambda_{dr}^{s}\\ \lambda_{qr}^{s}\end{bmatrix}=\frac{L_r}{L_m}\left[\begin{bmatrix}v_{ds}^{s}\\ v_{qs}^{s}\end{bmatrix}-\begin{bmatrix}R_s+\sigma L_s p & 0\\ 0 & R_s+\sigma L_s p\end{bmatrix}\begin{bmatrix}i_{ds}^{s}\\ i_{qs}^{s}\end{bmatrix}\right] \tag{41}$$

$$p\begin{bmatrix}\lambda_{dr}^{s}\\ \lambda_{qr}^{s}\end{bmatrix}=\begin{bmatrix}-1/T_r & -\omega_r\\ \omega_r & -1/T_r\end{bmatrix}\begin{bmatrix}\lambda_{dr}^{s}\\ \lambda_{qr}^{s}\end{bmatrix}+\frac{L_m}{T_r}\begin{bmatrix}i_{ds}^{s}\\ i_{qs}^{s}\end{bmatrix} \tag{42}$$

Figure 11 illustrates the structure of the proposed speed estimator of an induction motor using NNs. In Fig. 11, the voltage equations and the current equations are defined as Eqns. (41) and (42), respectively.

The voltage equations that do not involve ω_r is defined as the reference model and the current equations involving ω_r is defined as *the adjustable model*. The output of the ANNs is defined as the estimated speed $\hat{\omega}_r$, which is subsequently used as the input of the *adjustable model*. If the estimated speed deviates from the real speed, an error occurs between the flux from the adjustable model ($\hat{\lambda}_r$) and the flux from the reference model (λ_r). Then, the error

is backpropagated to the ANN and the weights of the NN are adjusted online to reduce the error. Finally, the output of the NN follows the real speed.

Methods based on ANN gives good speed estimation with parameter mismatch however, they are relatively complicated and require large computation time.

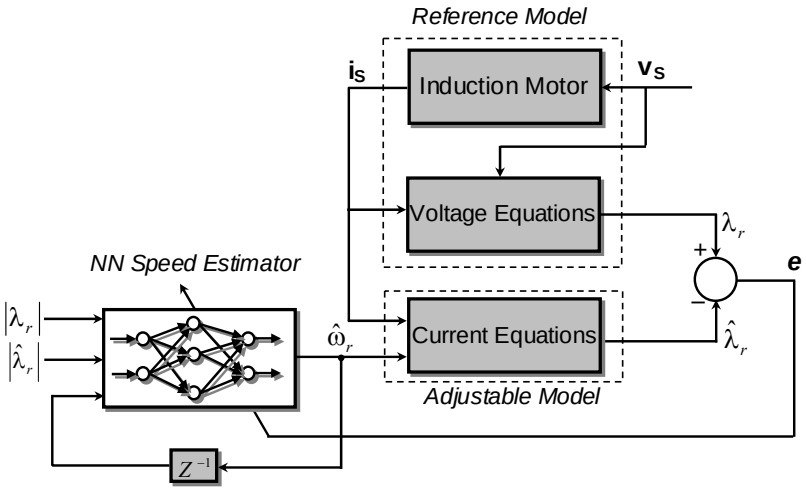

Fig. 11 Structure of the speed estimation using artificial Neural Network.

3.3.6. Sliding mode observer

Recently, there is a growing interest of using sliding mode observers (SMO) for speed estimation of induction motor drives. This observer is based on Variable Structure Control (VSC) theory which offers many good properties, such as good performance against un-modeled dynamics, insensitivity to parameter variations, external disturbance rejection and fast dynamic response. These properties are necessary for state estimation of a nonlinear plant such as speed estimation of induction motor drives. In spite the positive features of SMO, its application for speed estimation of induction motor drives requires chattering problem elimination [32-36].

The induction motor can be represented by its dynamic model expressed in the stationary reference frame in terms of the stator current and rotor flux by the following state equations;

$$\frac{d}{dt}\begin{bmatrix} i_s^s \\ \lambda_r^s \end{bmatrix} = \begin{bmatrix} a_{11} & a_{12} \\ a_{21} & a_{22} \end{bmatrix}\begin{bmatrix} i_s^s \\ \lambda_r^s \end{bmatrix} + \begin{bmatrix} b_1 \\ 0 \end{bmatrix}\left[u_s^s\right] = Ax + Bu_s \qquad (43)$$

where a_{11}, a_{12}, a_{21}, a_{22} and b_1 are given in the Appendix.

The SMO for rotor flux estimation can be constructed as:

$$\frac{d\hat{x}}{dt} = \hat{A}\hat{x} + Bu_s + K_1 \, sgn\left(\hat{i}_s^s - i_s^s\right) \tag{44}$$

Where K_1 is a gain matrix which can be arranged in the following general form;

$K_1 = [K \quad -K]^T$, $K = kI$ and k is the switching gain.

The equation of rotor speed estimation can be written in the following form based on Lyapunov theory:

$$\hat{\omega}_r = -k\int\left[sgn\left(\hat{i}_{ds}^s - i_{ds}^s\right)\cdot\hat{\lambda}_{qr}^s - sgn\left(\hat{i}_{qs}^s - i_{qs}^s\right)\cdot\hat{\lambda}_{dr}^s\right]dt \tag{45}$$

The structure of the sliding mode speed estimation algorithm is shown in Fig. 12.

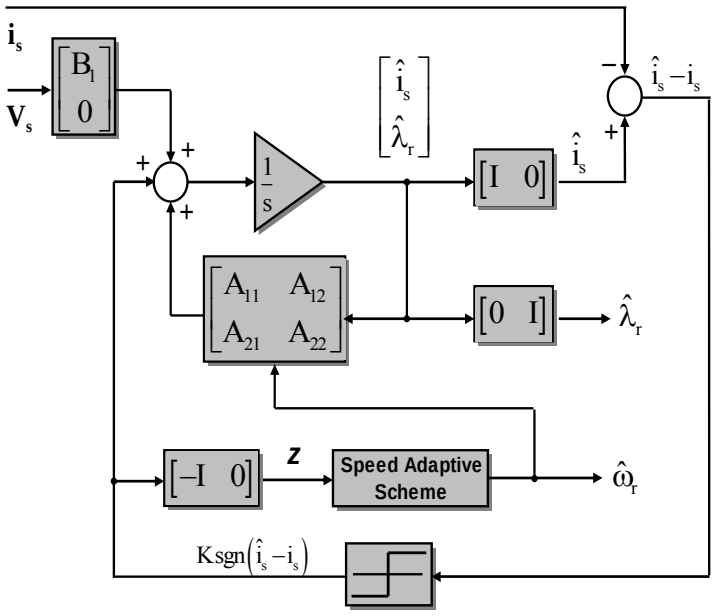

Fig. 12 Block diagram of sliding mode observer.

4. SPEED ESTIMATION AT LOW SPEED

The key problem in sensorless vector control of ac drives is the accurate dynamic estimation of the stator flux vector during wide speed range operation using only terminal variables (currents and voltages). The main difficulty consists on state estimation at very low speeds where the fundamental excitation is low and the observer performances tend to be

poor. The reasons are the observer sensitivity to model parameter variations, unmodeled nonlinearities and disturbances, limited accuracy of acquisition signals, drifts, and dc offsets. The main sources of poor speed estimation at low speed depend on three main problems [37-40].

4.1. Data Acquisition Errors

Data acquisition errors become significant at low speeds. That is because current sensors convert the machine currents to voltage signals which are subsequently digitized by A/D converters. Parasitic dc offset components are superimposed to analog signals and appear as ac components of fundamental frequency after their transformation to synchronous coordinates. They act as disturbances to the current control system, thus generating a torque ripple. The effect of unbalanced gains of the current acquisition channels is also another problem [5].

4.2. Voltage Distortion due the PWM Inverter

The task of the power inverter is to produce the desired voltage on the stator winding using PWM controlled switches. Since the switching times of the existing transistors are not infinitely short, the necessary blanking time to avoid short circuiting the dc link during commutations must be introduced, which is also known as dead time. This small time delay is the most important cause of the inverter nonlinearity and introduces a magnitude and phase error in the output-voltage vector. In addition to the dead time, there is also the finite voltage drop across the switch during the ON state, which introduces an additional error in the magnitude of the output voltage. Taking the inverter model into consideration enables a more accurate estimation of the stator flux linkage vector and consequently, good estimated speed is achieved [5, 38].

4.3. Stator Resistance Drop

In the upper speed range, the resistive voltage drop is small as compared with the stator

voltage; hence the stator flux vector and speed estimation can be made with good accuracy. At low speeds the stator frequency is also low. The stator voltage reduces almost in direct proportion, while the resistive voltage drop maintains its order of magnitude and becomes significant at low speed. The resistive voltage drop greatly influence the estimation accuracy of the stator flux vector and hence the speed estimation. On the other hand, considerable variations of the stator resistance are encountered when the machine temperature changes at varying load. These variations need to be tracked to maintain stability of flux estimation at low speed [5, 40].

Several methods to improve the low-frequency performance of the voltage model have been proposed. For example, the stator voltage and current can be measured more accurately, the voltage drop of the inverter can be compensated, and the stator resistance can be identified with an adaptive scheme, or the integrator itself can be modified to a low-pass filter [38-40].

5. PARAMETER ADAPTATION

Although machine model-based methods of speed estimation are characterized by their simplicity, one of the problems associated with them is their sensitivity to parameter variations. Stator resistance plays an important role and its value has to be known with good precision in order to obtain an accurate estimation of the rotor speed in the low speed region [41-44]. Since motor heating usually causes a considerable variation in the winding resistance, so there is often a mismatch between the actual winding resistance and its corresponding value in the model used for speed estimation. This may lead not only to a substantial speed estimation error but to instability as well. As a consequence, numerous online schemes for stator resistances identification have been proposed, recently [41-44]. The available online stator resistance identification schemes can be classified into a couple of distinct categories. All these methods rely on stator current measurements and chiefly require

information regarding stator voltages as well [45-49]. The most famous methods include different types of estimators which often use an adaptive mechanism to update the value of stator resistance [45-49]. The stator resistance is determined in [45] by using a reactive power based model reference adaptive system (MRAS). The reactive power relies on the accuracy of other parameters such as leakage inductance and rotor resistance which are not necessarily constant and the result is prone to error. Adaptive full-order flux observers (AFFO) for estimating the speed and stator resistance are developed using Popov's and Lyapunov stability criteria [46, 47]. While these schemes are not computationally intensive, an AFFO with a non-zero gain matrix may become unstable. Model reference adaptive system for estimating the speed and stator resistance is developed using Popov's stability criterion [48, 49]. In such methods, the stator resistance adaptation mechanism is determined with the difference between the measured and observed stator currents.

A wide speed range, with the maximum required speed that considerably exceeds the motor rated speed, is required for many applications such as spindle and gearless traction drives. Speed estimation in the field weakening region presents redoubtable difficulties regardless of the method used for the speed estimation. The main problem of machine model-based approaches in the field weakening region stems from the substantial variation of the magnetizing inductance as main flux saturation which is neglected in the model-based speed estimation. Therefore, accurate speed estimation in the field weakening region using model-based approaches is possible only if modifying the speed estimation algorithm in such a way that the variation of main flux saturation is recognized within the estimator [50-51].

A field oriented induction motor operates in the base speed region with constant rated rotor flux reference. Therefore, magnetizing inductance can be regarded as constant and equal to its rated value. The operation in field weakening region at higher speeds than the rated causes that the rotor flux reference has to be reduced below its rated value. Variation of the rotor

flux reference implies variable level of the main flux saturation in the machine and consequently, magnetizing inductance of the machine is a variable parameter [53-54]. Accurate value of magnetizing inductance is of utmost importance for many reasons. The first one is the correct setting of the d-axis stator current reference in a vector-controlled drive which requires the accurate magnetizing inductance value to be known. The second one is the accurate speed estimation, using machine model-based approaches, of a sensorless vector controlled drive for operation in the field-weakening region. The third reason is the dependency of rotor time constant identification schemes on magnetizing inductance such as the method of [53] which utilizes reactive power method. The accurate of rotor time constant estimation in the field weakening region requires that the value of the magnetizing inductance to be known correctly.

Many researches have been devoted to improve speed estimation of a field oriented controlled induction motor in constant flux operation region. However, the studies of magnetizing inductance identification to improve speed estimation in the field weakening region are still rarely made. In [52], the nonlinear magnetizing inductance is represented by a fitted quadratic polynomial of field current which is composed of three components, namely the no-load, the load compensating, and the transient compensating commands to give good dynamic response in both steady state and transient states. The method of magnetizing inductance identification used in [54] depends on measured stator voltages and currents and the magnetizing curve of the machine.

6. FINAL COMMENTS

Table 1 shows the comparison between the different speed estimation methods according to the set of criteria which has been chosen to assign the merits for each presented method. The criteria which are used to compare the different speed estimation methods include Steady

State Error (SSE), Dynamic Behavior (DB), Low Speed Operation (LSO), Parameter Sensitivity (PS), Noise Sensitivity (NS), Complexity (C), and Computation Time (CT). The range of merits is graded from 1 to 5, where 1 means the best behavior while 5 means the poorest one as shown in Table 2.

Table 1 Comparison of different speed estimation methods

Method \ Criteria		SSE	DB	LSO	PS	NS	C	CT
RST		**2**	**3**	**1**	**1**	**4**	**5**	**3**
FSI		**2**	**2**	**1**	**1**	**4**	**5**	**3**
MMM	DCM	**2**	**3**	**4**	**4**	**4**	**2**	**2**
	MRAS	**2**	**3**	**4**	**3**	**4**	**2**	**3**
	KF	**2**	**2**	**2**	**2**	**1**	**5**	**5**
	AFO	**2**	**1**	**3**	**3**	**2**	**2**	**2**
	AI	**1**	**1**	**2**	**1**	**2**	**3**	**4**
	SM	**1**	**1**	**2**	**1**	**2**	**2**	**2**

Table 2 Merits grade of speed estimation methods

Excellent	**Very good**	**Good**	**Satisfactory**	**Weak**
1	2	3	4	5

The present comparison is based on a comprehensive reading and investigation of the previous literature. Figure 13 shows a chart to compare the different speed estimation methods according to the adopted set of criteria. It is observed that, rotor slot harmonic and frequency signal injection methods are recommended when low speed operation is required. In drive systems which have many sources of noise, EKF is preferred since it is designed to perform as an optimal filter. Although Artificial Intelligence techniques exhibit good performance for most criteria, it suffers from complexity and large computation time. It is also noted that, SMO offers good behavior with respect to all proposed set of criteria.

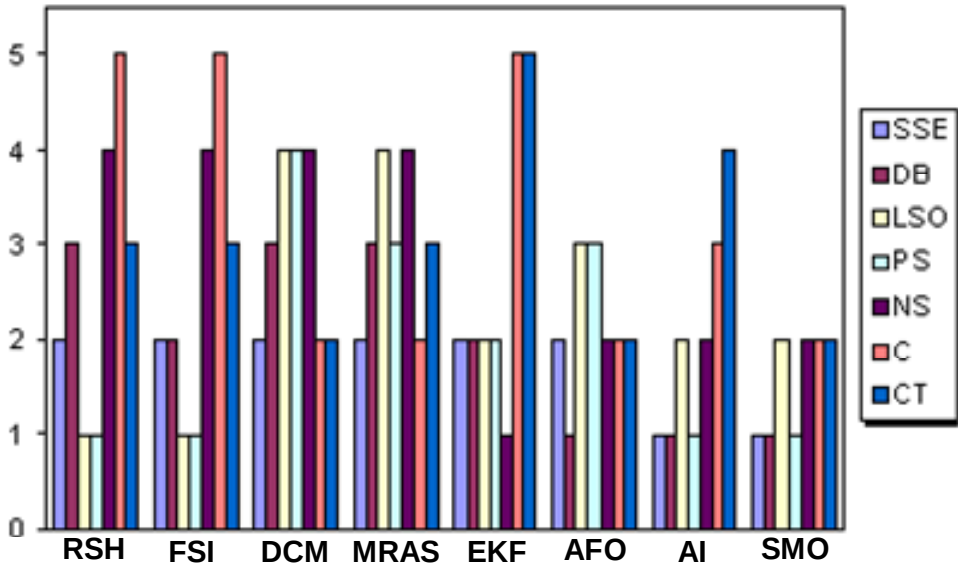

Fig. 13 Comparison chart for different speed estimation methods.

Some simulation and experimental results are necessary to prove the superiority of SMO. The previously mentioned mathematical model of speed estimation based on SMO, shown in Fig. 12, is firstly examined by simulation. Sensorless operation is investigated where the estimated speed is used instead the actual feedback one. The actual and estimated speeds are compared during starting operation. Figure 14 shows the actual and estimated speeds as well as speed estimation error during start up at speed command equal to 100 rad/sec. The speed estimation error is quite zero soon after 0.025 sec from starting, which illustrates the high accuracy and fast convergence of the SMO. The speed observer is also examined during starting operation in the low speed region with stator resistance adaptation scheme. Fig. 15 shows the actual and estimated speeds, and the speed estimation error with speed reference set at 1 rad/sec under no load condition. It is observed that, very good speed estimation is achieved and the speed estimation error rapidly decays to zero. The speed observer is capable of operation at zero speed, provided that the stator resistance in the estimator exactly matches the one in the motor. Fig. 16 shows the actual and estimated speeds as well as the speed estimation error at zero speed with stator resistance tuning. As shown, the proposed speed

observer with stator resistance adaptation achieves good speed estimation. Furthermore, the results confirm that due to the accurate stator resistance estimation, the drive does not loose stability during operation at very low and zero speeds. The correct value of the stator resistance leads to elimination of the speed estimation error and the actual and estimated speeds are in very good agreement in steady state.

Some of tests are performed experimentally in order to verify the accuracy of the speed observer. Figure 17 shows the experimentally actual and estimated speeds during start up operation for speed command equal to 150 rad/sec. Figure 18 shows the Actual and estimated speeds for a reversing transient from 100 to -100 rad/sec. As shown, good estimated speed during reversing transient through zero speed is achieved. Persistent operation at zero speed is possible experimentally as shown in Fig. 19 with stator resistance adaptation. The Experimental results confirm good speed estimation and the drive does not loose stability during temporary operation at zero speed with stator resistance adaptation.

The presented simulation and experimental results show that,

- No steady state error.
- Good speed estimation at low speed.
- Good dynamic behavior.
- Simple design of SMO and low computation time.
- Robustness of SMO.

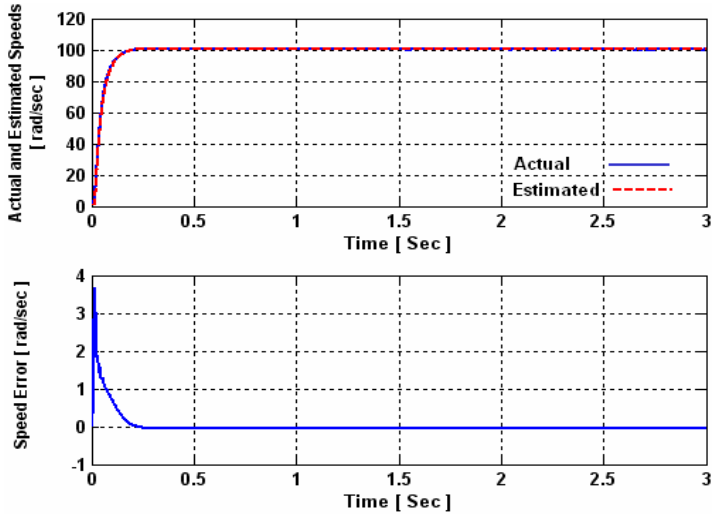

Fig. 14 Actual and estimated speeds, and speed estimation error during starting operation at speed command of 100 rad/sec.

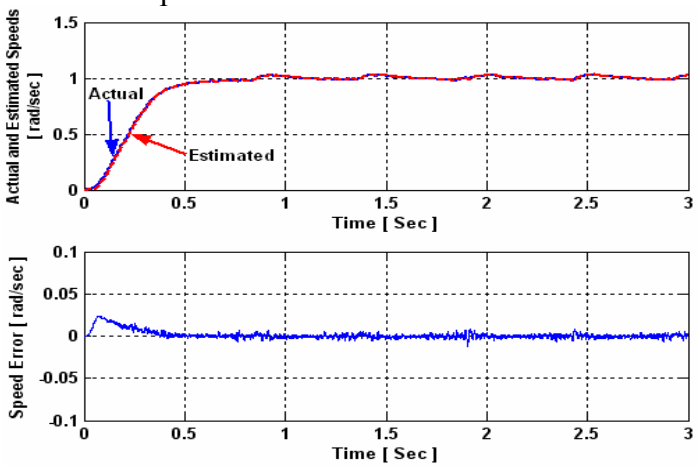

Fig. 15 Actual and estimated speeds, and speed estimation error during starting operation with stator resistance tuning at speed commands of 1 rad/sec.

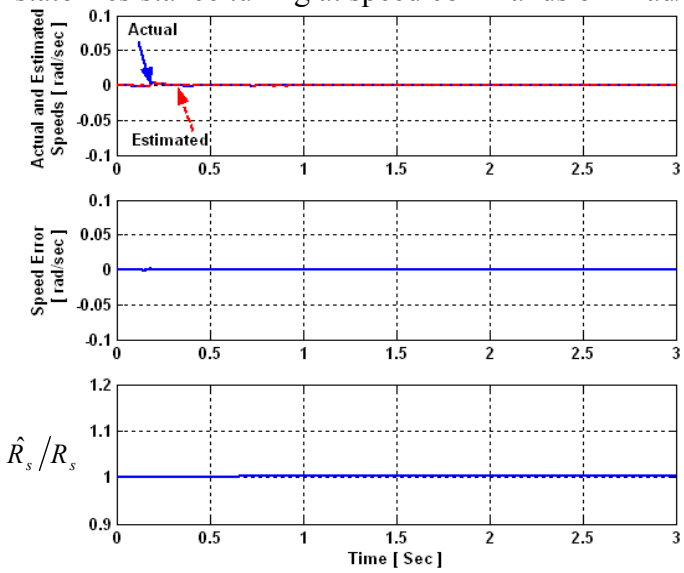

Fig. 16 Actual and estimated speeds, and speed estimation error with stator resistance tuning at zero speed.

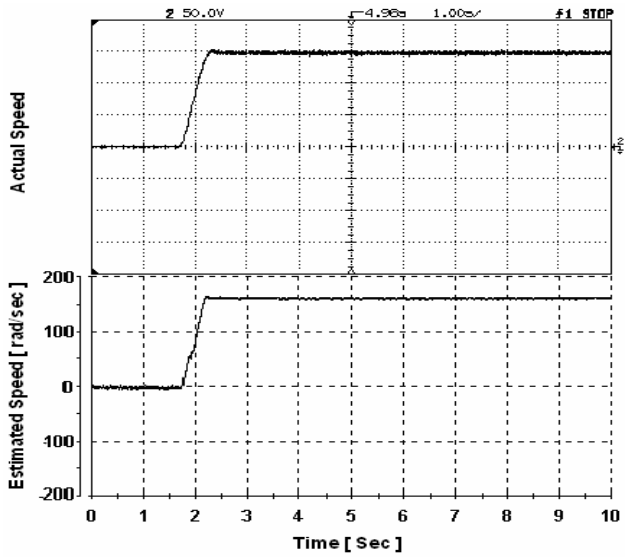

Fig. 17 Actual and estimated speeds during start up operation at 150 rad/sec

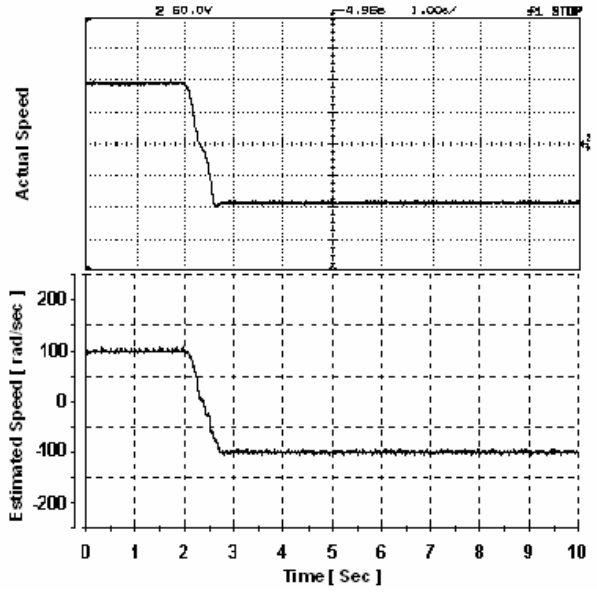

Fig. 18 Actual and estimated speed during speed reversal at 100 rad/sec.

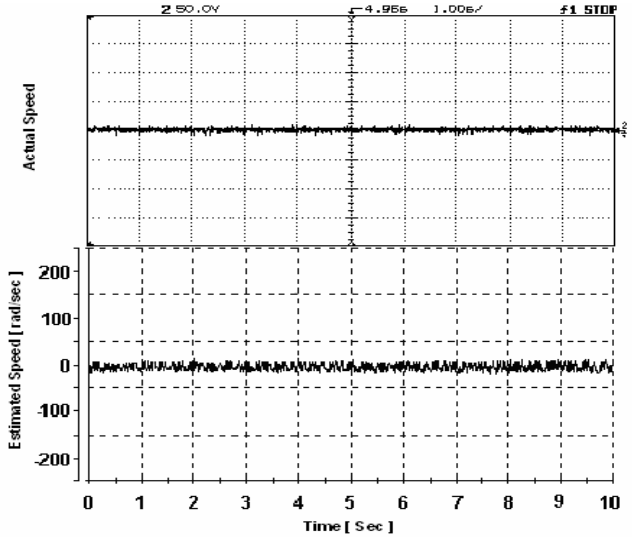

Fig. 19 Actual and estimated speed at zero speed.

7. CONCLUSION

A review of different schemes for speed sensorless induction motor drives has been presented and classified. The merits and demerits of these schemes are discussed. Many factors remain important to evaluate the effectiveness of the different schemes proposed for speed estimation. Among them are steady state error, dynamic behavior, noise sensitivity, low speed operation, parameter sensitivity, complexity, and computation time. It is concluded that, the rotor slot harmonic and signal injection methods are recommended when low speed operation is required. Among machine model-based methods, sliding mode observer seems to have the best behavior with respect to all the considered criteria. However, in a noisy environment, extended Kalman filter has the best behavior, since it is particularly designed to perform as optimal filtering.

Stator resistance plays an important role and its value has to be known with good precision in order to obtain accurate very low-speed and zero-speed estimations. In applications that requires speeds higher than the rated, accurate value of magnetizing inductance is of utmost importance for accurate speed estimation, using machine model-based approaches, in the field-weakening region

As a final comment, each speed estimation method of sensorless application requires a specific design, which takes into consideration the required performance, the available hardware and the designer skills.

8. APPENDIX

A. List of symbols

L_m	Mutual inductance
L_r	Rotor leakage inductance
L_s	Stator leakage inductance
R_s	Stator resistance
T_r	Rotor time constant
ω_r	Rotor angular speed
σ	Leakage coefficient
$i_s^s = [i_{ds}^s \quad i_{qs}^s]^T$	Stator current vector
$\hat{i}_s^s = [\hat{i}_{ds}^s \quad \hat{i}_{qs}^s]^T$	Estimated Stator current vector
$\lambda_r^s = [\lambda_{dr}^s \quad \lambda_{qr}^s]^T$	Rotor flux vector
$\hat{\lambda}_r^s = [\hat{\lambda}_{dr}^s \quad \hat{\lambda}_{qr}^s]^T$	Estimated rotor flux vector
$v_s^s = [v_{ds}^s \quad v_{qs}^s]^T$	Stator voltage vector
$\hat{\omega}_r$	Estimated rotor speed
$p = d/dt$	Differential operator
τ_{sl}	Filter time Constant
ω_s	Slip Angular Frequency

$$a_{11} = aI, \quad a_{12} = cI + dJ, \quad a_{21} = eI, \quad a_{22} = -\varepsilon a_{12}, \quad b_1 = bI$$

$$I = \begin{bmatrix} 1 & 0 \\ 0 & 1 \end{bmatrix}, \quad J = \begin{bmatrix} 0 & -1 \\ 1 & 0 \end{bmatrix}$$

$$a = -\left(\frac{R_s}{\sigma L_s} + \frac{L_m^2}{\sigma L_s T_r L_r}\right), \quad c = \frac{1}{\varepsilon T_r}, \quad d = \frac{\omega_r}{\varepsilon}, \quad e = \frac{L_m}{T_r}$$

$$\varepsilon = \frac{\sigma L_s L_r}{L_m}, \quad b = \frac{1}{\sigma L_s}, \quad \sigma = 1 - \frac{L_m^2}{L_s L_r}, \quad T_r = \frac{L_r}{R_r}$$

$$A_{11} = -\left(\frac{R_s}{\sigma L_s} I + \omega_r J\right), \; A_{12} = R_s \frac{(1-\sigma)}{\sigma L_m} I, \; A_{21} = R_r \frac{(1-\sigma)}{\sigma L_m} I,$$

$$A_{22} = \frac{-R_r}{\sigma L_r} I, \; B_1 = I, \; C = \left[\frac{1}{\sigma L_s} I \quad \frac{\sigma - 1}{\sigma L_m} I\right]$$

9. REFERENCES

1. Alfio Consoli, Giuseppe Scarcella, and Antonio Testa, Slip-Frequency Detection for Indirect Field-Oriented Control Drives. IEEE Trans. Ind. Applic., 40 (1) (2004), pp. 194-201.
2. Sheng-Ming Yang, and Shuenn-Jenn Ke, Performance evaluation of a velocity observer for accurate velocity estimation of servo motor drives. IEEE Trans. Ind. Applic., 36 (1) (2000), pp. 98-104.
3. Muhammed Fazlur Rahman, L. Zhong, Md. Enamul Haque, and M. A. Rahman, A Direct Torque-Controlled Interior Permanent-Magnet Synchronous Motor Drive Without a Speed Sensor. IEEE Trans. Energy Conversion, 18 (1) (2003), pp. 17-22.
4. Gautam Poddar and V. T. Ranganathan, Sensorless field-oriented control for double-inverter-fed wound-rotor induction motor drive. IEEE Trans. Ind. Electr., 51 (5) (2004), pp. 1089-1096.
5. Joachim Holtz, Sensorless Control of Induction Motor Drives. IEEE Proc., 90 (8) (2002), pp. 1359-1394.
6. C. Ilas, A. Bettini, L. Ferraris, G. Griva, and F. Profumo, Comparison of different schemes without shaft sensors for field oriented control drives. IEEE Conf. in the Ind. Electr. (IECON'94), 3 (1994), pp. 1579-1588.

7. Mohsen Elloumi, Lazhar Ben-Brahim and Mohamed A. Al-Hamadi, Survey of speed sensorless controls for IM drives. Proc. of the 24th Annual Conf. of the IEEE Ind. Electr. (IECON'98), 2/4 (1998), Aachen, Germany, pp. 1018-1023.
8. Cyril Spiteri Staines, Greg M. Asher, and Mark Sumner, Rotor-position estimation for induction machines at zero and low frequency utilizing zero-sequence currents. IEEE Trans. Ind. Applic., 42 (1) (2006), pp. 105-112.
9. Cyril Spiteri Staines, Cedric Caruana, Greg M. Asher, and Mark Sumner, Sensorless Control of Induction Machines at Zero and Low Frequency Using Zero Sequence Currents. IEEE Trans. Ind. Electr., 53 (1) (2006), pp. 195-206.
10. Marko Hinkkanen, Veli-Matti Leppänen, and Jorma Luomi, Flux observer enhanced with low-frequency signal injection allowing sensorless zero-frequency operation of induction motors. IEEE Trans. Ind. Applic., 41 (1) (2005), pp. 52-59.
11. Mihai Comanescu, and Longya Xu, An Improved Flux Observer Based on PLL Frequency Estimator for Sensorless Vector Control of Induction Motors. IEEE Trans. Ind. Electr., 53 (1) (2006), pp. 50-56.
12. Alfio Consoli, Giuseppe Scarcella, Giovanni Bottiglieri, Giacomo Scelba, Antonio Testa, and Domenico Antonino Triolo, Low-Frequency Signal-Demodulation-Based Sensorless Technique for Induction Motor Drives at Low Speed. IEEE Trans. Ind. Electr., 53 (1) (2006), pp. 207-215.
13. Veli-Matti Leppänen and Jorma Luomi, Observer Using Low-Frequency Injection for Sensorless Induction Motor Control—Parameter Sensitivity Analysis. IEEE Trans. Ind. Electr., 53 (1) (2006), pp. 216-224.
14. Joachim Holtz, Sensorless Control of Induction Machines—With or Without Signal Injection. IEEE Trans. Ind. Electr., 53 (1) (2006), pp. 7-30.

15. C. Schauder, Adaptive speed identification for vector control of induction motor without rotational transducers. IEEE Trans. Ind. Applic., 28 (5) (1992), pp. 1054–1061.
16. M. N. Marwali and A. Keyhani, A comparative study of rotor flux based MRAS and back EMF based MRAS speed estimators for speed sensorless vector control of induction machines. Proc. of the IEEE-IAS Annual Meeting, 1997, pp. 160–166.
17. F.Z. Peng, T. Fukao, Robust speed identification for speed-sensorless vector control of induction motors. IEEE Trans. Ind. Applic., 30 (5), 1994, pp. 1234–1240.
18. M. Rashed and A.F. Stronach, A stable back-EMF MRAS-based sensorless low speed induction motor drive insensitive to stator resistance variation. IEE Proc. Electr. Power Applic., 151 (6) (2004), pp. 685-693.
19. Chul-Woo Park and Woo-Hyen Kwon, Simple and robust speed sensorless vector control of induction motor using stator current based MRAC. Electric Power Systems Research, Elsevier, 71 (2004), pp. 257–266.
20. G. Garcia Soto, E. Mendes and A. Razek, Reduced-order observers for rotor flux, rotor resistance and speed estimation for vector controlled induction motor drives using the extended Kalman filter technique. IEE Proc.-Electr. Power Applic., 146 (3)(1999), pp. 282-288.
21. J. K. AI-Tayie and P. P. Acarnley, Estimation of speed, stator temperature and rotor temperature in cage induction motor drive using the extended Kalman filter algorithm. IEE Proc. Electr. Power Applic., 144 (5) (1997), pp. 301-309.
22. Malik E. Elbuluk and M. David Kankam, Speed sensorless induction motor drives for electrical actuators: schemes, trends and tradeoffs. National Aerospace and Electr. Conf., IEEE, Dayton, Ohio, July 14-18, 1997, pp. 1-8.

23. Jehudi Maes and Jan A. Melkebeek, Speed-Sensorless direct torque control of induction motors using an adaptive flux observer. IEEE Trans. Ind. Applic., 36 (3) (2000), pp. 778-785.

24. Marko Hinkkanen, Analysis and design of full-order flux observers for sensorless induction motors. IEEE Trans. Ind. Electr.,. 51 (5) (2004), pp. 1033-1340.

25. Hisao Kubota, Ikuya Sato, Yuichi Tamura, Kouki Matsuse, Hisayoshi Ohta, and Yoichi Hori, Regenerating-mode low-speed operation of sensorless induction motor drive with adaptive observer. IEEE Trans. Ind. Applic., 38 (4) (2002), pp. 1081-1086.

26. Cristian Lascu, Ion Boldea, and Frede Blaabjerg, Comparative study of adaptive and inherently sensorless observers for variable-speed induction-motor drives. IEEE Trans. Ind. Electr., 53 (1) (2006), pp. 57-65.

27. Surapong Suwankawin and Somboon Sangwongwanich, Design strategy of an adaptive full-order observer for speed-sensorless induction-motor drives—tracking performance andstabilization. IEEE Trans. Ind. Electr., 53 (1) (2006), pp. 96-119.

28. J. Campbell and M. Sumner, Practical sensorless induction motor drives employing an artificial neural network for online parameter adaptation. IEE Proc. Electr. Power Applic., 149 (4) (2000), pp. 255-260.

29. Jordi Català i López, Luis Romeral, Antoni Arias, and Emiliano Aldabas, Novel Fuzzy Adaptive Sensorless Induction Motor Drive. IEEE Trans. Ind. Electr., 53 (4) (2006), pp. 1170-1178.

30. J. R. Heredia, F. Perez Hidalgo, and J. L. Duran Paz, Sensorless Control of Induction Motors by Artificial Neural Networks. IEEE Trans. Ind. Electr., 48 (5) (2001), pp. 1038-1040.

31. Seong-Hwan Kim, Tae-Sik Park, Ji-Yoon Yoo, and Gwi-Tae Park, Speed-sensorless vector control of an induction motor using neural network speed estimation. IEEE Trans. Ind. Electr., 48 (3) (2001), pp. 609-614.
32. Jingchuan Li, Longya Xu, and Zheng Zhang, An adaptive sliding-mode observer for induction motor sensorless speed control. IEEE Trans. Ind. Applic., 41 (4) (2005), pp. 1039-1046.
33. Adnan Derdiyok, Speed-sensorless control of induction motor using a continuous control approach of sliding-mode and flux observer. IEEE Trans. Ind. Electr., 52 (4) (2005), pp. 1170-1176.
34. Gregor Edelbaher, Karel Jezernik, and Evgen Urlep, Low-speed sensorless control of induction machine. IEEE Trans. Ind. Electr., 53 (1) (2006), pp. 120-129.
35. Cristian Lascu and Gheorghe-Daniel Andreescu, Sliding-mode observer and improved integrator with DC-offset compensation for flux estimation in sensorless-controlled induction motors. IEEE Trans. Ind. Electr., 53 (3) (2006), pp. 785-794.
36. M. M. Khater, M. S. Zaky, H. Yasin, S. S. Shokralla, and A. El-Sabbe, A Comparative Study of Sliding Mode and Model Reference Adaptive Speed Observers for Induction Motor Drives. MEPCON'2006, El-Minia, Egypt, 2 (2006), pp. 434-440.
37. Alfio Consoli, Giuseppe Scarcella, and Antonio Testa, Speed- and current-sensorless field-oriented induction motor drive operating at low stator frequencies. IEEE Trans. Ind. Applic., 40 (1) (2004), pp. 186-193.
38. Joachim Holtz, and Juntao Quan, Sensorless vector control of induction motors at very low speed using a nonlinear inverter model and parameter identification. IEEE Trans. Ind. Applic., 38 (4) (2002), pp. 1087-1095.
39. Hirokazu Tajima, Giuseppe Guidi, and Hidetoshi Umida, Consideration about problems and solutions of speed estimation method and parameter tuning for speed-sensorless

vector control of induction motor drives. IEEE Trans. Ind. Applic., 38 (5) (2002), pp. 1282-1289.

40. Joachim Holtz, and Juntao Quan, Drift- and Parameter-Compensated Flux Estimator for Persistent Zero-Stator-Frequency Operation of Sensorless-Controlled Induction Motors. IEEE Trans. Ind. Applic., 39 (4) (2003), pp. 1052-1060.
41. Veran Vasic, Slobodan N. Vukosavic, and Emil Levi, A stator resistance estimation scheme for speed sensorless rotor flux oriented induction motor drives. IEEE Trans. Energy Conversion, 18 (4) (2003), pp. 476-483.
42. Giuseppe Guidi, and Hidetoshi Umida, A Novel Stator Resistance Estimation Method for Speed-Sensorless Induction Motor Drives. IEEE Trans. Ind. Applic., 36 (6) (2000), pp. 1619-1627.
43. Mineo Tsuji, Shuo Chen, Katsuhiro Izumi, and Eiji Yamada, A Sensorless Vector Control System for Induction Motors Using q-Axis Flux with Stator Resistance Identification. IEEE Trans. Ind. Electr., 48 (1) (2001), pp. 185-194.
44. Juan Luis Zamora and Aurelio Garcia-Cerrada, Online estimation of the stator parameters in an induction motor using only voltage and current measurements. IEEE Trans. Ind. Applic., 36 (3) (2000), pp. 805-816.
45. Gregor Edelbaher, Karel Jezernik, and Evgen Urlep, Low-speed sensorless control of induction machine. IEEE Trans. Ind. Electr.,. 53 (1) (2006), pp. 120-129.
46. Hossein Madadi Kojabadia, and Liuchen Changb, "Comparative study of pole placement methods in adaptive flux observers. Control Engineering Practice, Elsevier, 13 (2005), pp. 749–757.
47. Jehudi Maes and Jan A. Melkebeek, Speed-Sensorless direct torque control of induction motors using an adaptive flux observer. IEEE Trans. Ind. Applic., 36 (3) (2000), pp. 778-785.

48. Mdaadi Kojabadi, H., Simulation and experimental studies of model reference adaptive system for sensorless induction motor drive. Simulation Modeling Practice and Theory, Elsevier, 13 (2005), pp. 451–464.

49. Veran Vasic, Slobodan N. Vukosavic, and Emil Levi, A stator resistance estimation scheme for speed sensorless rotor flux oriented induction motor drives. IEEE Trans. Energy Conversion, 18 (4) (2003), pp. 476-483.

50. Myoung-Ho Shin, and Dong-Seok Hyun, "Speed Sensorless Stator Flux-Oriented Control of Induction machine in the Field Weakening Region," IEEE Trans. on Power Electr., Vol. 18, No. 2, March 2003, pp. 580-586.

51. Tae-Sung Kwon, Myoung-Ho Shin, and Dong-Seok Hyun, "Speed Sensorless Stator Flux-Oriented Control of Induction Motor in the Field Weakening Region Using Luenberger Observer," IEEE Trans. on Power Electr., Vol. 20, No. 4, July 2005, pp. 864-869.

52. M. S. Wang, and C. M. Liaw, "Improved Field-Weakening Control for IFO Induction Motor" IEEE Trans. on Aerospace and Electronic Systems, Vol. 39, No. 2, April 2003, pp. 647-658.

53. Emil Levi, and Mingyu Wang, "A Speed Estimator for High Performance Sensorless Control of Induction Motors in the Field Weakening Region," IEEE Trans. on Power Electr., Vol. 17, No. 3, May 2002, pp. 365-378.

54. Emil Levi, and Mingyu Wang, "Online Identification of the Mutual Inductance for Vector Controlled Induction Motor Drives," IEEE Trans. on Energy Conversion, Vol. 18, No. 2, June 2003, pp. 299-305.